IEEE Access
Multidisciplinary | Rapid Review | Open Access Journal

Received August 24, 2020, accepted September 27, 2020, date of publication October 13, 2020, date of current version October 27, 2020.

*Digital Object Identifier 10.1109/ACCESS.2020.3030843*

# Two-Phase Current Injection Method for Single Line-to-Ground Fault Arc-Suppression With Revised STATCOM

**YANGMING CHEN [1], SHUAI LU [1], (Member, IEEE), XINGDA ZHOU [2], (Member, IEEE), AND SHIBIN LIANG [3]**

[1]School of Electrical Engineering, Chongqing University, Chongqing 400044, China
[2]Institute of Science and Technology, China Three Gorges Corporation, Beijing 100038, China
[3]Yunnan Electric Power Test and Research Institute Company, Ltd., Kunming 650217, China

Corresponding author: Shuai Lu (lushuai1975@gmail.com)

**ABSTRACT** To suppress the arc current in the single line-to-ground (SLG) fault in neutral isolated distribution network, a two-phase current injection method is proposed for the revised static synchronous compensator (STATCOM), as an extra function during the SLG fault. Therefore, the traditional roles of the dedicated passive coil or power electronic based arc-suppression devices can be taken by this multi-purpose STATCOM. This article first introduces the principles and the models of the arc-suppression current injection during SLG fault. Then, different options of arc-suppression current injection by the revised STATCOM are analyzed in terms of stabilizing the floating dc capacitor voltages of the cascaded H-bridges (CHB) converter. It is discovered that the two-phase current injection is the only viable option to maintain the floating dc capacitors voltages. Then, the arc-suppression current controller and the dc capacitors voltages controller are proposed, and the design process of the control parameters adapting to the varying transitional (grounding) resistances computed online is also introduced. The proposed methods are first validated by simulations. Then, an MVA-rating CHB converter prototype is constructed, and 10 kV feeder SLG fault and arc-suppression experiments are performed to demonstrate the effectiveness of the proposed method.

**INDEX TERMS** Single line-to-ground (SLG) fault, arc suppression, cascaded H-bridge (CHB) converter, floating dc capacitor voltage control.

## NOMENCLATURE

(X and Y present A, B, or C; *n* presents 0, 1, 2...)

| | |
|---|---|
| $\dot{E}_X$ | Per-phase voltage of phase X |
| $\dot{U}_{XY}$ | Line voltage between the phase X and Y |
| $\dot{U}_{Xg}$ | Line-to-ground voltage of phase X |
| $\dot{U}_X$ | Voltage output of CHB phase X |
| $\dot{U}_0$ | Neutral displacement voltage |
| $\dot{I}_{X0}$ | Parasitic capacitive current of phase X |
| $\dot{I}_{Xs}$ | Injected arc-suppression current to phase X |
| $\dot{I}_S$ | Total injected arc-suppression current |
| $\dot{I}_f$ | Ground-fault current |
| $R_f$ | Transitional (grounding) resistance |
| $R_k$ | Equivalent line resistance per phase |
| $L_k$ | Equivalent line inductance per phase |
| $L_S$ | Converter filter inductance per phase |
| $C_0$ | Lumped parasitic capacitance to earth per phase |
| $C_{dc}$ | Floating dc capacitance of each H-bridge cell |
| $S_n$ | High-voltage switches |

The associate editor coordinating the review of this manuscript and approving it for publication was B. Chitti Babu.

## I. INTRODUCTION

With the growing scale of the distribution networks, its reliable operation becomes more challenging [1], [2]. The single line-to-ground (SLG) faults are the dominant failures in the distribution networks [3], [4]. If the fault current is not suppressed shortly, the arc is induced, and the line-to-ground voltage of the two non-faulty phases will be boosted to the value of the line voltage during a permanent SLG fault. This could lead to insulation failure and subsequent short circuits between two lines [5]–[8]. Therefore, suppressing the SLG fault current quickly is of vital importance for the reliable operation of distribution networks. However, with the increase usage of power cables, significant amount of parasitic capacitive current from the two non-faulty phases makes it very difficult to suppress the SLG fault current.

Nowadays, the passive arc-suppression method has been widely used in the power distribution networks [9], [10]. When the SLG fault occurs, the Petersen Coil or arc-suppression coil (ASC) connected to the neutral point of the feeder side of the substation transformer induces the compensating current to eliminate the fault arc. However, the bulky Petersen coil is hard to configure the proper parameters to induce accurate amount of compensating current, due to the changing parameters of the growing distribution network [11], [12]. Alternatively, the phase earthing system (PES) could be applied to divert the capacitive current to ground to extinguish the arc at the SLG fault point [13]–[15]. Basically, the faulty phase is selected and grounded via the shunt circuit breaker installed on the feeder side bus bar. Although the PES is a straightforward solution, it would induce the resonance overvoltage. Several measures have been presented to achieve dynamic adjustment of the parameters of the passive ASC for accurate arc-suppression current. An adaptive arc-suppression coil with the use of capacitor and resistor units connected in parallel has been presented in [16] to reduce the active and reactive currents in the zero-sequence circuit, yet it still cannot get the stepless adjustment of compensation current.

Power electronics based active ac-suppression methods are proposed in [17]–[20]. In [17]–[19], inverters based current sources are connected to the neutral point. Therefore, all the active, reactive and harmonic components of the ground fault current can be dynamically compensated. The hybrid Petersen coil is presented in [20], where an active power compensator (APC) is added in parallel with the ASC. Therefore, the arc current can be accurately compensated with reduced power electronic usage. All these active ac-suppression options [17]–[20] connect to the neutral point of the feeder side of the transformer and dedicated dc sources are needed. Note that an equivalent neutral point could be created by a zigzag transformer connected to the 3-phase bus bar, if the transformer feeder side is delta-connected. Alternatively, it is possible to directly connect the arc-suppression device to the feeder side 3-phase output of the transformer as introduced in [21], [22], where a cascaded H-bridges (CHB) multilevel converter is used. However, isolated dc sources are required to maintain all the dc capacitor voltages of numerous H-bridge cells. Therefore, 380 V lab results as in [22] cannot be extended to the practical applications. Obviously, a practical arc-suppression current injection method is needed to balance the floating dc capacitors voltage in between all three phases and then all the cascaded H-bridge cells per-phase. Also, the proposed method must be experimentally validated with the 10 kV rated distribution network testbed.

This article proposes a two-phase current injection based flexible grounding method with no need for numerous floating dc sources. In Section II, it is introduced that the revised static synchronous compensator (STATCOM) is connected to the feeder side bus bar of the substation, and the other ends of the three converter legs are individually grounded in case of a SLG fault. When the distribution network operates normally, the converter's neutral point is floated. In case of SLG fault, the relationship between the various options of arc-suppression current injection and the floating dc capacitor voltage control of the CHB converter is analyzed. It is discovered that arc-suppression currents injected into the two non-faulty phases will not disturb the voltage balance of the numerous floating dc sources between phases. Then in Section III, the arc-suppression current controller and the dc capacitors voltages controller are proposed, and the design process of the control parameters adapting to the varying transitional (grounding) resistances computed online are also introduced. Section IV provides the simulations results. In Section V, an MVA rating prototype of the revised STATCOM is constructed and the feasibility of the proposed two-phase current injection based flexible grounding method is experimentally verified at 10 kV distribution network. Finally, Section VI concludes the paper.

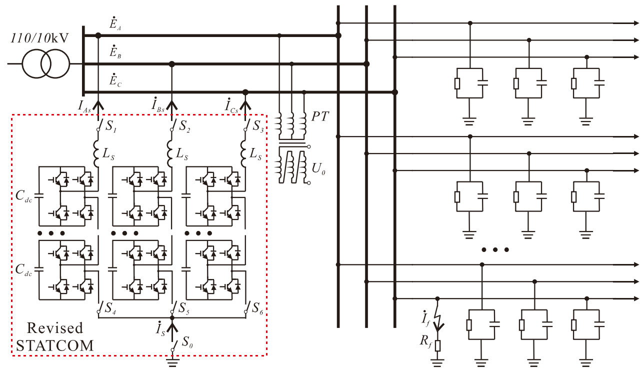


**FIGURE 1. General configuration of the distribution network with the revised STATCOM.**

## II. PRINCIPLE OF THE PROPOSED TWO-PHASE ARC-SUPPRESSION CURRENT INJECTION METHOD

### A. MODEL OF THE DISTRIBUTION NETWORK WITH THE REVISED STATCOM

A general configuration of the distribution network with the revised STATCOM is shown in Fig. 1. The CHB-converter-based STATCOM is directly connected to the transformer feeder side bus bar via output filter inductors. Seven high-voltage switches are used to configure the CHB converters to different operating mode. The neutral displacement voltage is detected online by the potential transformer ($PT$). SLG fault occurs on the phase $C$, and the ground-fault current $\dot{I}_f$ flows through a transitional (grounding) resistor $R_f$.

### B. ANALYSIS OF THE ARC-SUPPRESSION CURRENT

When SLG fault occurs, the revised STATCOM enters the arc suppression mode and starts to inject the compensation current. Herein, the output current can be individually regulated for each phase leg of CHB. Therefore, in the equivalent circuit

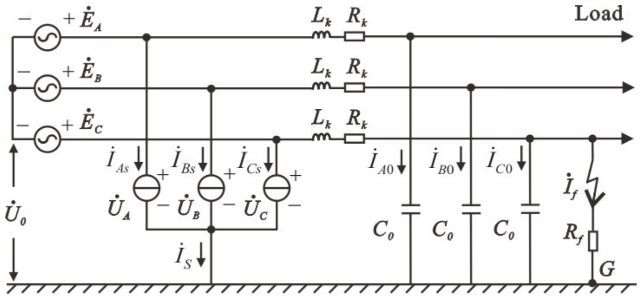


**FIGURE 2.** **Equivalent circuit of the distribution network with the revised STATCOM.**

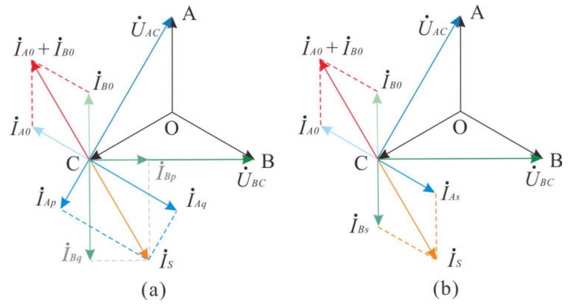


**FIGURE 3.** **Phasor relationship between the injected arc-suppression current and the phase voltages. (a) the single phase (A or B) injection current. (b) the two-phase injection current to Phase A and B.**

of the distribution network in Fig. 2, the revised STATCOM can be simplified as three individually controlled current sources. The current flowing into the ground (node $G$) is assumed as positive.

When SLG fault occurs at C-phase feeder line as illustrated in Fig. 2, the capacitive currents of the non-faulty phase A and B would flow through the transformer neutral point onto the C-phase, and then enters the SLG fault point. Hence, the capacitive current ($\dot{I}_{A0} + \dot{I}_{B0}$) induce and sustain the arc. Zero transitional resistance is assumed for now, so that $\dot{I}_{C0}$ is zero. Therefore, the arc-suppression principle is to divert the capacitive currents of the non-faulty phases ($\dot{I}_{A0} + \dot{I}_{B0}$) from the fault point to a different grounding point. In essence, the conventional ASC connecting the neutral point to ground is to intercept $\dot{I}_{A0} + \dot{I}_{B0}$ and divert it to the ground before it goes to the C-phase feeder line. As for the revised-STATCOM connected at the transformers' feeder side bus bar, it also intercepts $\dot{I}_{A0} + \dot{I}_{B0}$ and routes it into the ground by the additional grounding switch $S_0$ in Fig. 1. Obviously, the current can be routed to the ground via A, B, C, A+B, B+C, A+C or all 3-phase legs of the CHB converters. The current can be individually regulated by the 3-phase legs of CHB converters and summed up to suppress arc. Therefore, the total arc-suppression current can be derived as

$$\dot{I}_S = -\left(\dot{I}_{A0} + \dot{I}_{B0}\right) \tag{1}$$

which can be further expanded as

$$\begin{cases} \dot{I}_S = \dfrac{3\dot{E}_C - \dot{I}_f(Z_0 + 2Z_f)(j\omega C_0 R_f + 1)}{Z_0} \\ Z_0 = j\omega L_k + R_k + \dfrac{1}{j\omega C_0} \\ Z_f = j\omega L_k + R_k + \dfrac{R_f}{1 + j\omega C_0 R_f} \end{cases} \tag{2}$$

where $\dot{E}_A + \dot{E}_B + \dot{E}_C = 0$, and $\omega = 2\pi f_g$($f_g$ is the grid frequency).

To suppress the ground-fault current $\dot{I}_f$ to zero, the required arc-suppression current $\dot{I}_S$ is obtained from (2) as

$$\dot{I}_S = \frac{3\dot{E}_C}{j\omega L_k + R_k + \frac{1}{j\omega C_0}} \tag{3}$$

The required arc-suppression current in the steady state is not dependent on the transitional resistance $R_f$ at the fault point, as (3) is derived assuming the ground-fault current is zero, $\dot{I}_f = 0$. This assumption might seem not correct, since the fault current through the transitional resistance introduces extra voltage at the fault point. Therefore, the faulty phase voltage, neutral displacement voltage and the non-faulty phases line-to-ground voltages will all be altered and the capacitive current expressions will be different than (3), before arc-suppression current injection starts. Despite the complications from the unpredictable transitional resistances, the arc-suppression current (3) can still be safely used as the control target. This would not completely compensate the whole capacitive current at the start, but it reduces the fault current and increases the neutral displacement voltage, so that the total capacitive current gets closer to the value defined by (3). Obviously, this process will rapidly converge to total cancellation of the fault current and zero voltage at the fault point, no matter what transitional resistances there are.

As the parasitic capacitance of the feeder lines has much larger reactance value than those from the line inductances and resistances, equation (3) can be further simplified as

$$\dot{I}_S = 3\dot{E}_C j\omega C_0 \tag{4}$$

### *C. THE PROPOSED TWO PHASES ARC-SUPPRESSION CURRENT INJECTION METHOD*

Theoretically, the arc-suppression current can be injected by one, two or three phase legs of the STATCOM, as long as the total injected current reaches the value defined by (4). However, as the floating dc capacitor banks are used for each H-bridge cell of the CHB converter, the impacts of different current injection options on the dc capacitors voltage regulation has to be analyzed, so that the CHB converter can function normally during the arc-suppression mode.

As in prior discussion, despite the unpredictable transitional resistances, the capacitive current will soon converge to the arc-suppression current target. Then, the line-to-ground voltage of faulted phase is clamped to zero, and the line-to-ground voltages of two non-faulty phases become line voltages. Consequently, the phasor relationship between the injected arc-suppression currents and the phase voltages can be illustrated in Fig. 3.

According to Fig. 2, if the total arc-suppression current is injected to the non-faulty phase A, $\dot{I}_S$ and the total capacitive current $\dot{I}_{A0} + \dot{I}_{B0}$ should have the equal value and opposite directions. So as illustrated in Fig. 3(a), the $\dot{I}_S$ and $\dot{U}_{AC}$ will not be perpendicular, and $\dot{I}_S$ will have the active $\dot{I}_{Ap}$ part besides the reactive $\dot{I}_{Aq}$. Note that $\dot{I}_{Ap}$ is opposite to $\dot{U}_A$; in other words, if the CHB converter injects the whole arc-suppression current to the non-faulty phase A, active powers will keep charging all the floating dc capacitors of the A-phase of the CHB converter, so that the capacitor voltage cannot be stabilized.

As for the non-faulty phase B case, it can be similarly illustrated as in Fig. 3(a) that there has to be an active component $\dot{I}_{Bp}$ with the same direction as $\dot{U}_{BC}$, indicating that the active power is depleting the dc capacitors in the B-phase of the CHB converter. In the case that the total arc-suppression current is injected to the faulted phase C, the phase voltage is clamped to zero. Therefore, this arc-suppression mode will have no impacts (active power flow) on regulating the dc capacitor voltages of each H-bridge cells. According to the prior analysis, if the total arc-suppression current is injected simultaneously by the three CHB converter phase legs (equally split), the dc capacitors voltages of the three phase legs will be not stabilized particularly for the non-faulty phase A and B. In summary, using single phase leg of the CHB or all three phase legs of the CHB to inject the arc-suppression current will not be feasible in practice, since the numerous floating dc capacitors of the CHB converter will not have the stabilized voltages.

Therefore, the two-phase arc-suppression current injection method is proposed in this article. Herein, $S_1$, $S_4$, $S_2$, $S_5$, $S_0$ as in Fig. 1 are closed, and $S_3$, $S_6$ are opened. As in Fig. 3(b), the current is injected by the CHB converter into the two non-faulty phases. The total arc-suppression current $\dot{I}_S$ is the vector sum of $\dot{I}_{As}$ and $\dot{I}_{Bs}$, which are opposite to $\dot{I}_{A0}$ and $\dot{I}_{B0}$, respectively. As $\dot{I}_{A0}$ and $\dot{I}_{B0}$ are capacitive and are perpendicular to $\dot{U}_{AC}$ and $\dot{U}_{BC}$, respectively, the injected current $\dot{I}_{As}$ and $\dot{I}_{Bs}$ are also reactive. Hence, two proposed two-phase arc-suppression current injection method will maintain the dc capacitors voltages stability. The arc-suppression current injection reference value is defined as

$$\begin{cases} \dot{I}_{As} = -\dot{U}_{AC} j\omega C_0 = -(\dot{E}_A - \dot{E}_C) j\omega C_0 \\ \dot{I}_{Bs} = -\dot{U}_{BC} j\omega C_0 = -(\dot{E}_B - \dot{E}_C) j\omega C_0 \\ \dot{I}_S = \dot{I}_{As} + \dot{I}_{Bs} \end{cases} \tag{5}$$

## III. CONTROL STRATEGY OF THE PROPOSED TWO-PHASE INJECTION METHOD

As for the revised STATCOM, the control of reactive power compensation mode is mature technology, so that only the proposed two-phase arc-suppression current injection method is discussed here. When SLG fault occurs, the current control loop of the two-phase legs (A and B) of the CHB converter can be controlled separately. So the A-phase leg of the CHB converter is used to explain the controller design for the arc-suppression current. The simplified circuit is displayed in Fig. 4.

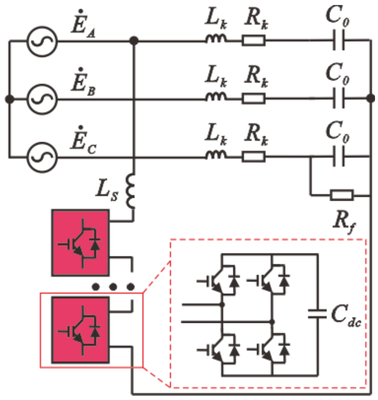


**FIGURE 4.** Circuit of one phase leg (phase A) in the CHB converter.

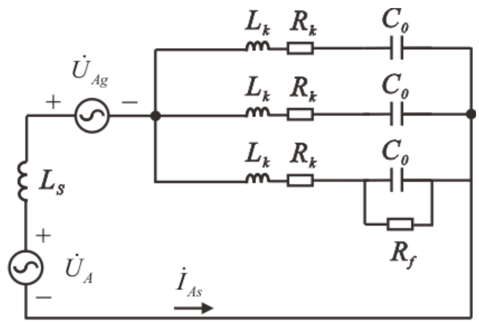


**FIGURE 5.** Equivalent circuit of one phase leg (phase A) in the CHB converter.

There are two control objectives for the arc-suppression current controller as explained in the subsequent subsections. One is to dynamically regulate the arc-suppression current target, and the other is to maintain stable dc capacitors voltages of H-bridge cells during the arc-suppression mode.

### A. ARC-SUPPRESSION CURRENT REGULATOR

The circuit in Fig. 4 can be simplified into the equivalent circuit as in Fig. 5, where the CHB converter is equivalent to a voltage source in series with a filter inductor. To design the arc-suppression current regulator, the transfer function from the equivalent voltage $\dot{U}_A$ to the injected current $\dot{I}_{As}$ has to be obtained.

As shown in Fig. 5, $\dot{U}_{Ag}$ is the line-to-ground voltage of phase A. As there is a transitional resistance, $\dot{U}_{Ag}$ is not equal to $\dot{E}_A$ when SLG fault occurs. Actually, $\dot{U}_{Ag}$ is measured online at the feeder bus and used as a feedforward term for the design of the arc-suppression current loop controller.

The transfer function from the equivalent voltage $\dot{U}_A$ to the injected current $\dot{I}_{As}$ is derived as

$$G_1(s) = \frac{I_{As}(s)}{U_A(s)} = -\frac{Z_0(s) + 2Z_f(s)}{Z_0(s)Z_f(s) + sL_S(Z_0(s) + 2Z_f(s))} \tag{6}$$

As the arc-suppression current controller regulates the single-phase alternating current, the quasi-proportional-resonant (PR) controller together with a proportional gain

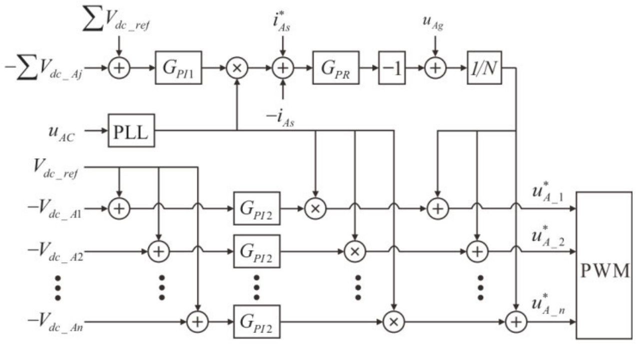


**FIGURE 6.** Control block diagram of the A-phase CHB converter.

$K$ can be used to achieve a sufficient gain at the resonance frequency, and it's expressed as

$$G_{PR}(s) = K\left(K_p + \frac{2K_r\omega_i s}{s^2 + 2\omega_i s + \omega_0^2}\right) \tag{7}$$

where $\omega_0$ is the resonance frequency of the controller, $\omega_i$ is the cutoff frequency, $K_r$ is the integral gain of the controller and $K_p$ is the proportional gain of the controller. The design process of the PR controller parameters $K$, $K_p$, $K_r$, $\omega_i$ and $\omega_0$ will be explained in the subsequent subsection C.

### B. VOLTAGE-BALANCING CONTROL

Even though the prior discussion of the proposed two-phase arc-suppression current injection method explained that there is no net active power flow from or to the floating dc capacitors, in practice, there is some power loss in each H-bridge cell while the arc-suppression current is injected. Therefore, the proposed arc-suppression current controller needs to meet the objective of regulating each floating dc capacitor voltages of the CHB converter, so that slight amount of active power is commanded in and out of each H-bridge cell. The transfer functions for the overall dc voltages and individual dc voltage models can be simply defined as

$$G_2(s) = \frac{1}{NC_{dc}s} \tag{8}$$

$$G_3(s) = \frac{1}{C_{dc}s}, \tag{9}$$

respectively, where $N$ is the number of H-bridge unit per phase leg.

Fig. 6 is the proposed overall control block diagram for the phase leg A (or B). $i^*_{As}$ and $i_{As}$ is the reference and the feedback of the arc-suppression current, respectively. $V_{dc\_ref}$ and $V_{dc\_An}$ are the reference and the feedback of the dc capacitor voltage of each H-bridge cell, respectively. The sum of all the dc capacitor voltages is controlled in closed loop by (10) and its output superposes onto the arc-suppression current target value. Then, the output of the PR current regulator is further divided by $N$. Then by adding the individual H-bridge cell dc capacitor voltage PI controller (11) output, the reference voltages for each H-bridge cell are obtained as $u^*_{A\_n}$.

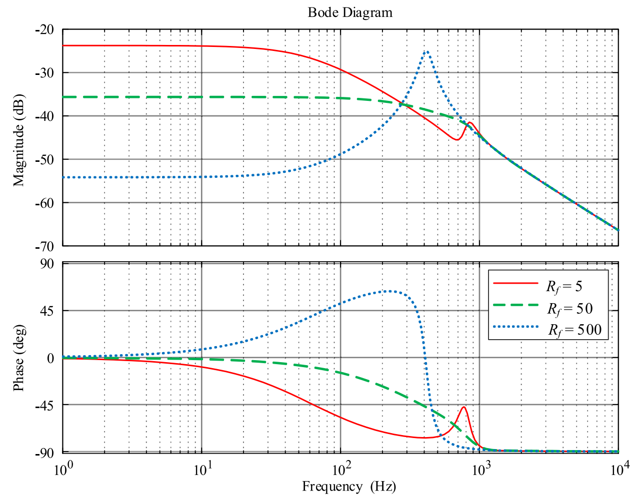


**FIGURE 7.** Bode diagrams of $G_1(s)$ as $R_f$ varies.

$$G_{PI1} = K_{p1} + \frac{K_{i1}}{s} \tag{10}$$

$$G_{PI2} = K_{p2} + \frac{K_{i2}}{s} \tag{11}$$

### C. CONTROLLER PARAMETERS DESIGN

The parameters of the distribution system with the revised STATCOM in Fig. 1 are listed in Table 2. With the open loop transfer function (6), the Bode diagrams under different transitional resistances are shown in Fig. 7. Obviously, as the value of the transitional resistance increases, the gain in the low-frequency region becomes smaller, rendering the system less stable. Therefore, the controller parameters in (7) should adapt to different transitional resistances.

For the application of this article, the resonance frequency is set to be the grid fundamental frequency, i.e. $\omega_0 = 2\pi f_g$; $\omega_i$ is usually set to be $\pi$ in order to reduce sensitivity to slight frequency variation in a typical grid. $K_r$ can be tuned for shifting the magnitude response in the resonance frequency, $K_p$ determines the dynamics of the system, and $K$ adjusts both characteristics. All three gains can be determined according to the Bode diagrams. Particularly, with the complication of the varying transitional resistances, the parameters $K$ varies accordingly, such that $K(R_f = 5\ \Omega) = 80$, $K(50\ \Omega) = 180$ and $K(500\ \Omega) = 580$. Herein, the parameters of $K_p$, $K_r$, $\omega_i$ and $\omega_0$ remain the same as in Table 1, despite different transitional resistances. Fig. 8 shows that the arc suppression current control is equally effective for different transitional resistances, as their gains at the resonant 50 Hz are kept as high as 40 dB. Then, the look-up table of the parameter $K$ can be built to adjust the control parameters in real-time, according to the transitional resistance computed online right after SLG fault occurs.

In practice, the equivalent circuit for the online transitional resistance $R_f$ computation can be illustrated in Fig. 9. Then,

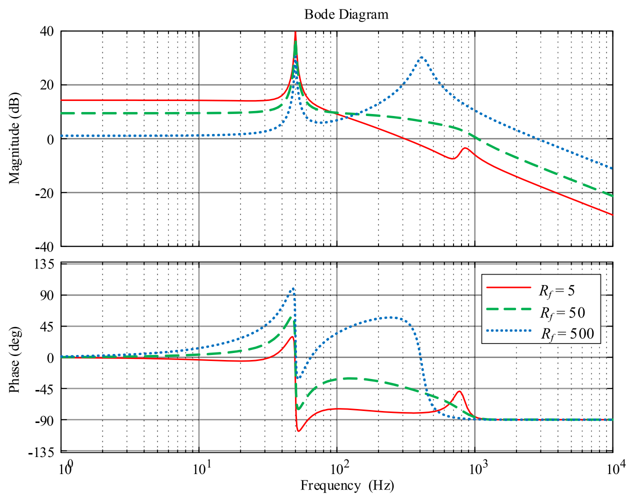


**FIGURE 8.** Bode diagrams of $G_{PR}(s)G_1(s)$ as $R_f$ varies.

**TABLE 1.** Controller parameters.

| Items | Value | Items | Value |
|---|---|---|---|
| $K_p$ | 1 | $K_{p1}$ | 0.01 |
| $K_r$ | 23 | $K_{i1}$ | 0.05 |
| $\omega_i$ | 3.14 | $K_{p2}$ | 0.001 |
| $\omega_0$ | 314 | $K_{i2}$ | 0.0005 |

the transitional resistance $R_f$ is computed as

$$R_f = \left| \frac{\dot{U}_{Cg}\frac{Z_0}{2} - (\frac{3}{2}\dot{E}_C - \dot{U}_{Cg})(j\omega L_k + R_k)}{(\frac{3\dot{E}_C}{2} - \dot{U}_{Cg})[1 + j\omega C_0(j\omega L_k + R_k)] - j\omega C_0 \dot{U}_{Cg}\frac{Z_0}{2}} \right| \tag{12}$$

where $\dot{U}_{Cg}$ is measured online at the feeder bus.

The bandwidth of the dc capacitors voltage control loops is generally set to be much lower than the current control loop. Since the minimum bandwidth of the arc-suppression current control loops is about 300 Hz, the bandwidths of the overall dc capacitors voltage control loop and the voltage balancing control loop as in Fig. 6 can be set to be less than 30 Hz and 3 Hz, respectively. Thereby, a set of optimal parameters for the two dc voltage control loops are also summarized in Table 1.

In practice, the distribution system feeder's parameters are measured and stored periodically during the distribution network normal operation. So that the controller parameters are obtained and updated regularly.

### D. CONTROL FLOW

Based on the above analysis, the control flow chart of the proposed two-phase arc-suppression injection method during SLG fault is shown in Fig. 10. When the value of the neutral point displacement voltage exceeds 15% of the amplitude of the power supply voltage, it indicates a SLG fault. Then, with

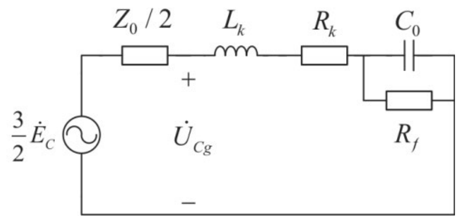


**FIGURE 9.** The equivalent circuit while measuring the transitional resistance.

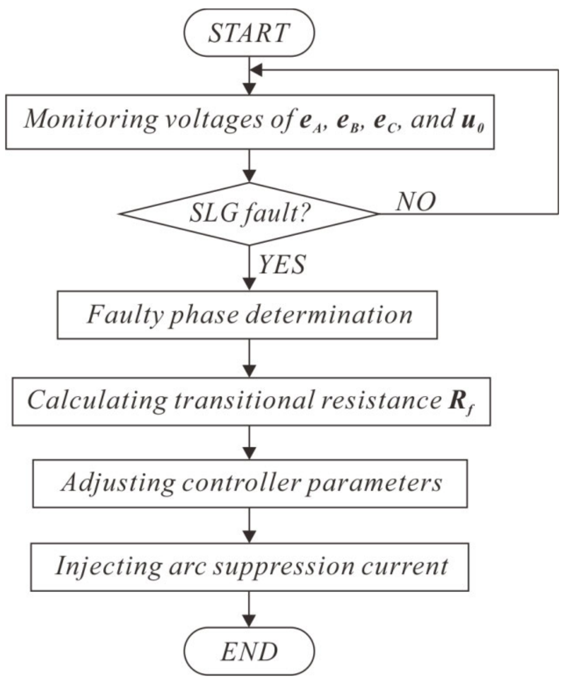


**FIGURE 10.** Control flow of the proposed two-phase arc-suppression current injection method.

the distribution network automation system, the faulted phase is determined, then the transitional resistance is calculated online with the neutral point displacement voltage measured online. According to the look-up table, the parameter $K$ is looked up from the table built offline. Then, the effective arc-suppression current is injected into the two non-faulty phases by the revised STATCOM.

## IV. SIMULATIONS

Matlab/Simulink was used to simulate the proposed two-phase arc-suppression current injection method. The parameters of the distribution network with the revised STATCOM as in Fig. 1 are listed in Table 2.

### A. ONLINE MEASUREMENT OF TRANSITIONAL RESISTANCE

When SLG occurs, the transitional resistance needs to be computed online as in (12). A transitional resistance of 192 Ω is used to create the SLG fault in the simulation. Then, with the feedbacks of the line-to-ground voltage of faulted phase, as in Fig. 11, the transitional resistance is computed online

**TABLE 2.** Distribution network parameters for both simulation and experiments.

| Items | Parameters | Value |
|---|---|---|
| *Distribution network* | $U_{XY}$ | 10.0 kV |
| | Grid frequency $f_g$ | 50 Hz |
| | $L_k$ | 9.8 mH |
| | $R_k$ | 10.4 Ω |
| | $C_0$ | 1.5 μF |
| | $R_f$ | 192 Ω |
| | Length of the feeder | 40 km |
| *Revised STATCOM* | STATCOM nominal power | 1 MVA |
| | $V_{dc\_ref}$ (per H-bridge cell) | 850 V |
| | $C_{dc}$ (per H-bridge cell) | 0.84 mF |
| | $L_S$ | 30 mH |
| | Number of H-bridge cells: $N$ | 20 |
| | Switching frequency (per H-bridge) $f_{sw}$ | 1 kHz |
| | Sampling frequency $f_s$ | 10 kHz |

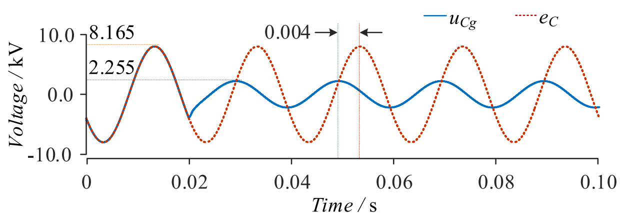


**FIGURE 11.** Waveform of the line-to-ground voltage of faulted phase and the supply voltage of faulted phase.

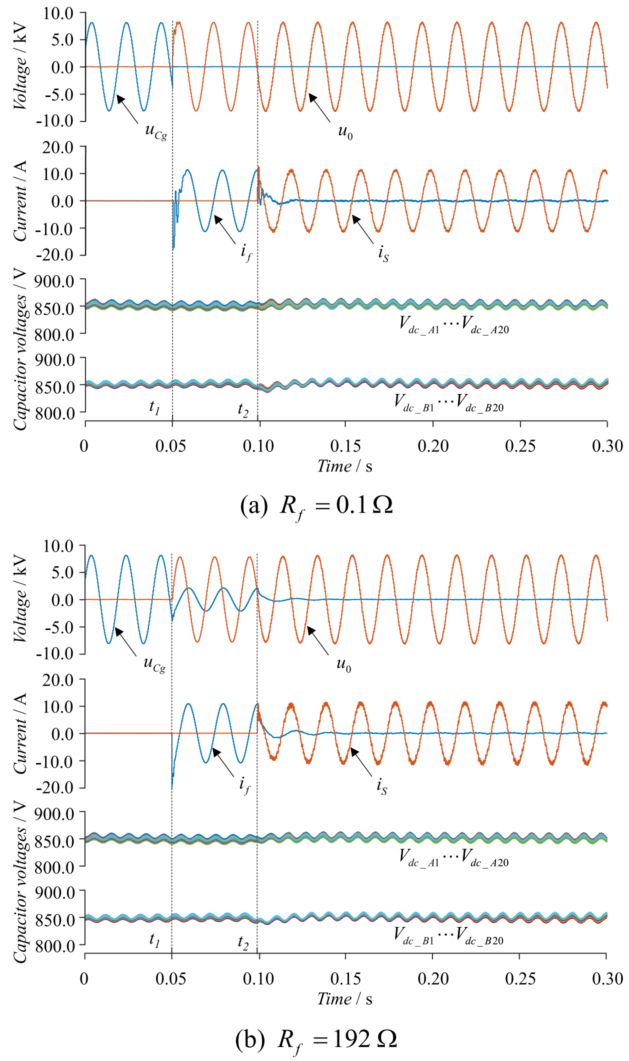


**FIGURE 12.** Simulation results of $\dot{U}_{Cg}$, $\dot{U}_0$, $\dot{I}_f$, $\dot{I}_S$ and the floating dc capacitor voltages with (a) $R_f = 0.1$ Ω, (b) $R_f = 192$ Ω.

as 195.42 Ω, which well matches the actual value. With the transitional resistance, the parameters $K$ is looked up as 290.

### B. SIMULATION ANALYSIS

In order to verify the effectiveness of the proposed two-phase injection method for SLG fault arc-suppression, both the metallic SLG fault ($R_f = 0.1$ Ω) and the resistive SLG fault ($R_f = 192$ Ω) are simulated. The results are shown in Figs. 12.

When t = $t_1$, Phase C grounds through transitional resistors (0.1 Ω or 192 Ω) to simulate a SLG, the increase of the neutral point displacement voltage $u_0$ exceeds the set threshold (15% of the phase voltage), which indicates the SLG detection.

When t = $t_2$, the arc-suppression current is injected from the A and B phase legs of the CHB, the well-tuned current regulator instantly output the arc-suppression current, so that the ground-fault current is rapidly diminished. For the metallic grounding fault, the peak ground-fault current is suppressed from 11.75 A to below 0.2 A. For the resistive grounding fault, the peak ground-fault current is suppressed from 11.15 A to less 0.1 A. From Fig. 12, it is noted that the steady-state arc-suppression currents are identical for both the metallic and the resistive grounding fault, which is consistent with the analysis in Section II.B Accordingly, the line-to-ground voltage of faulted phase is clamped to zero, and the neutral displacement voltage (opposite to the phase voltage of faulted phase C) is stabilized.

The two lower subplots in Fig. 12(a) and Fig. 12(b) shows the floating dc capacitor voltages of one H-bridge cell for Phase A and B, respectively. The dc capacitor voltage set point is 850 V. It is shown that there is no net active power flow with the proposed two-phase arc-suppression current injection method, so that the subsequent dc voltage regulation loops can easily stabilize the dc capacitors voltages during the entire arc suppression process. Also note that the second order harmonics are apparent over the dc capacitor voltage, which is typical in the dc-link of any CHB H-bridge cell.

## V. EXPERIMENTAL RESULTS

In order to verify the proposed two-phase injection method, an MVA-rated CHB converter prototype and a 10 kV

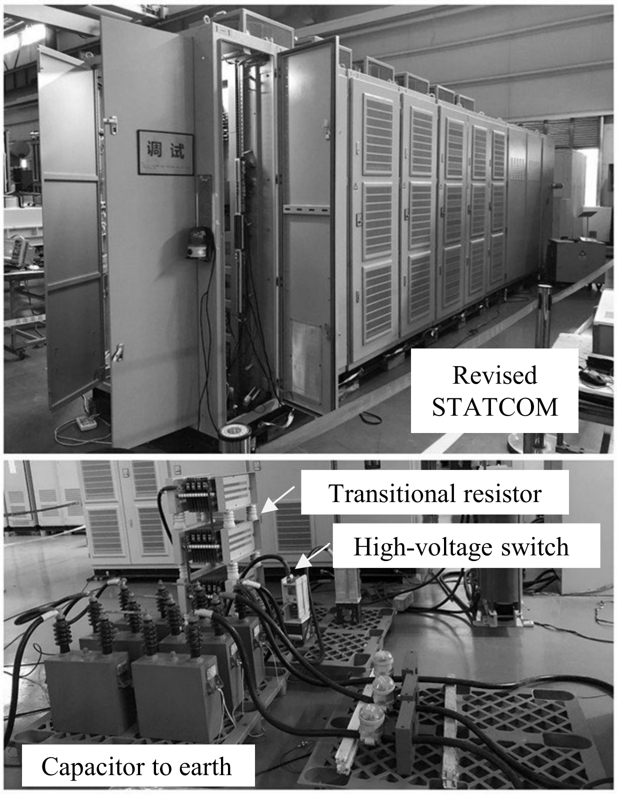


**FIGURE 13.** **The 10 kV prototype and the experimental setup.**

distribution network experimental platform has been developed according to Fig. 1, with the same parameters as in Table 2. The prototype and experimental setup are shown in Fig. 13. The 10 kV revised STATCOM prototype consists of three CHB phase legs, and each has cascaded twenty individual H-bridge cells. The reactive power compensation capacity of the revised STATCOM prototype is 1 MVA, so that the arc-suppression current injection capacity of each phase leg is up to 60 A. AC capacitor banks are used to emulate the lumped parasitic capacitance of the feeders to the ground. The proposed control strategy was implemented in a digital signal processor TMS320F2812 in combination with FPGA. Arrays of PWM signals are sent over fiber optic cables to each IGBT-based H-bridge cell. The same set of control parameters (Table 1) are used in the lab prototype as used in the prior simulations.

To analyze the effectiveness of the proposed arc-suppression method using the non-faulty phases A and B of CHB to inject the arc-suppression current, experiments under different transitional resistances (0 Ω or 192 Ω) were carried out. The waveforms in Fig. 14 are from the automatic oscillography Yokogawa DL850E, and the zoom-in views of the dotted regions are plotted with the recorded data. The 4 traces in Fig. 14 are the line-to-ground voltage of phase C $u_{Cg}$, the ground-fault current $i_f$, and the arc-suppression currents injected to two non-faulty phases $i_{As}$ and $i_{Bs}$, respectively.

In Fig. 14(a), while phase C is grounded via a 0 Ω resistor, ground fault current flows into the grounding point, and the

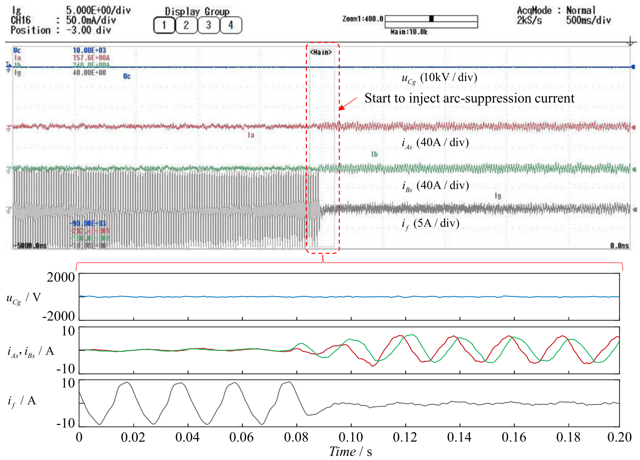


(a) $R_f = 0\ \Omega$

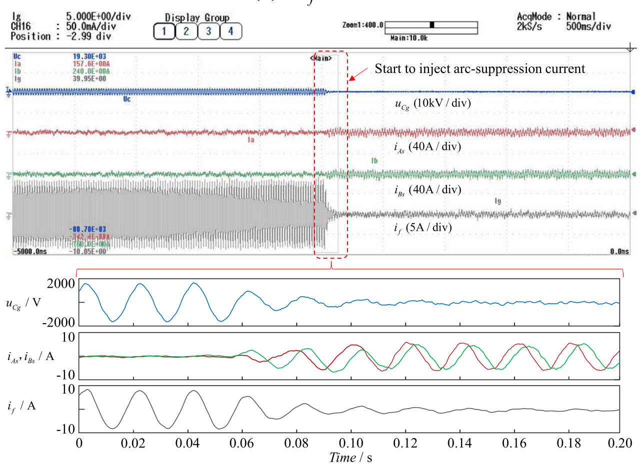


(b) $R_f = 192\ \Omega$

**FIGURE 14.** **Experimental results of $\dot{U}_{Cg}$, $\dot{I}_S$($\dot{I}_{As}$ and $\dot{I}_{Bs}$), $\dot{I}_f$, with (a) $R_f = 0.1\ \Omega$, (b) $R_f = 192\ \Omega$.**

C phase line-to-ground voltage is zero. With the well-tuned current regulator, the arc-suppression currents are instantly injected from the phase legs A and B of CHB converter, so that the ground-fault current is rapidly reduced to almost zero, i.e. the injected arc-suppression currents converges to the reference value as computed by (4).

Fig. 14(b) shows the SLG fault arc suppression waveforms when $R_f = 192\ \Omega$. With the current regulator adapting to the online computed transitional resistance, the arc-suppression current also reduces the SLG fault current to nearly zero. Compared to Fig. 14(a), there is more convergence time (less than 100 ms) for the fault current to diminish, since the initial capacitive current to be compensated at the start of the arc-suppression are not the same as the reference value by (4). This has been explained in Section 2.B, and also predicted by the simulations.

Meanwhile, the line-to-ground voltage of phase C starts with the value of the voltage drop of the fault current over the transitional resistance; then it converges to zero with the diminishing fault current, as the capacitive current converges to the arc-suppression currents.

## VI. CONCLUSION

During the distribution system SLG fault, it is necessary to suppress the arc induced by the parasitic capacitive currents from the two non-faulty phases. CHB based STATCOM can be revised to take the extra role of arc-suppression, which is conventionally done by dedicated passive ASC or power electronic based active arc-suppression devices. The prior attempts had to use many isolated dc power supplies for CHB even for the 380 V experimental test bed. Therefore, to make it possible to apply arc-suppression with the CHB tied to the busbar at the distribution system voltages (10 kV for example), the voltages of numerous floating capacitor banks in CHB have to be stabilized. The proposed two-phase arc-suppression current injection method guarantees that no net active power flows to/from any phase leg of CHB, so that all the floating capacitor voltages can be well regulated at the target. Then, an MVA-rating CHB converter prototype is constructed, and 10 kV SLG fault and arc-suppression experiments are successfully performed. Moreover, the paper also contributes some fresh insights into the arc-suppression process, and arc-suppression current regulator design process is also introduced that adapts to varying transitional (grounding) resistances.

## REFERENCES


[1] M. Rošer and G. Štumberger, "Improving the power supply reliability in resonant earthed systems by fault current path control established through faulted phase earthing switch," *Int. J. Electr. Power Energy Syst.*, vol. 64, pp. 714–722, Jan. 2015.

[2] J. Sinclair and I. Gray, "Assessing the potential for arc suppression coil technology to reduce customer interruptions and customer minutes lost," in *Proc. IET Conf. Publications*, Prague, Czech Republic, 2009, pp. 1–4.

[3] M. Vaziri and D. R. Smith, "Grounding of primary system for LV networks," *IEEE Trans. Power Del.*, vol. 31, no. 2, pp. 419–427, Apr. 2016.

[4] H. Yang, J. Tang, H. Hou, X. Wu, and X. Bian, "A novel zero-residual-current arc suppression method using single-phase voltage source inverter," in *Proc. IEEE Innov. Smart Grid Technol. Asia (ISGT Asia)*, Chengdu, China, May 2019, pp. 2042–2046.

[5] X. Lin, J. Huang, and S. Ke, "Faulty feeder detection and fault self-extinguishing by adaptive petersen coil control," *IEEE Trans. Power Del.*, vol. 26, no. 2, pp. 1290–1291, Apr. 2011.

[6] A. Cerretti, F. M. Gatta, A. Geri, S. Lauria, M. Maccioni, and G. Valtorta, "Ground fault temporary overvoltages in MV networks: Evaluation and experimental tests," *IEEE Trans. Power Del.*, vol. 27, no. 3, pp. 1592–1600, Jul. 2012.

[7] Y. Li, X. Song, and X. Meng, "Application of signal processing and analysis in detecting single line-to-ground (SLG) fault location in high-impedance grounded distribution network," *IET Gener., Transmiss. Distrib.*, vol. 10, no. 2, pp. 382–389, Feb. 2016.

[8] S.-R. Nam, S.-H. Kang, S.-J. Ahn, and J.-H. Choi, "Single line-to-ground fault location based on unsynchronized phasors in automated ungrounded distribution systems," *Electr. Power Syst. Res.*, vol. 86, pp. 151–157, May 2012.

[9] D. Topolanek, M. Lehtonen, P. Toman, J. Orsagova, and J. Drapela, "An earth fault location method based on negative sequence voltage changes at low voltage side of distribution transformers," *Int. J. Elect. Power Energy Syst.*, vol. 118, Jun. 2020, Art. no. 105768, doi: 10.1016/j.ijepes.2019.105768.

[10] H. Zeng, P. Yang, H. Cheng, J. Xin, W. Lin, W. Hu, M. Wan, Y. Li, and H. Wu, "Research on single-phase to ground fault simulation base on a new type neutral point flexible grounding mode," *IEEE Access*, vol. 7, pp. 82563–82570, 2019.

[11] L. Jian, T. Xiaozhuo, L. Yunge, Z. Zhihua, and L. Yu, "Analysis of arc suppression performance of active transfer type arc extinguishing device," in *Proc. Int. Conf. Power Syst. Technol. (POWERCON)*, Guangzhou, China, Nov. 2018, pp. 3614–3619.

[12] A. Kalyuzhny, "Analysis of temporary overvoltages during open-phase faults in distribution networks with resonant grounding," *IEEE Trans. Power Del.*, vol. 30, no. 1, pp. 420–427, Feb. 2015.

[13] A. Nikander, "Development of modern phase earthing system for improving quality of supply in the MV network," *IEEE Trans. Power Del.*, vol. 32, no. 3, pp. 1228–1235, Jun. 2017.

[14] M. Gonzalez, "Improvement of Saidi and Saifi reliability indices using a shunt circuit-breaker in ungrounded MV networks," in *Proc. 22nd Int. Conf. Exhib. Electr. Distrib. (CIRED )*, Stockholm, Sweden, 2013, pp. 112–115.

[15] K. Chen and X. Xiao, "Variable impedance fault current bypass circuit for fault arc suppression in distribution network," *IET Gener., Transmiss. Distrib.*, vol. 13, no. 18, pp. 4214–4221, Sep. 2019.

[16] Y. N. Ryzhkova, E. P. Mladzievskii, and S. A. Tsyruk, "Development of multifunctional adaptive resonance neutral grounding device," in *Proc. Int. Conf. Ind. Eng., Appl. Manuf. (ICIEAM)*, Sochi, Russia, Mar. 2019, pp. 1–6.

[17] K. M. Winter, "The RCC ground fault neutralizer—A novel scheme for fast Earth-fault protection," in *Proc. 18th Int. Conf. Exhib. Electr. Distrib. (CIRED)*, Truin, Italy, 2005, pp. 1–4.

[18] W. Wang, X. Zeng, L. Yan, X. Xu, and J. M. Guerrero, "Principle and control design of active ground-fault arc suppression device for full compensation of ground current," *IEEE Trans. Ind. Electron.*, vol. 64, no. 6, pp. 4561–4570, Jun. 2017.

[19] K. Chen, W. Zhang, and X. Xiao, "Faulted terminal open circuit voltage controller for arc suppression in distribution network," *IET Gener. Transmiss. Distrib.*, vol. 14, no. 14, pp. 5487–5494, May 2020.

[20] W. Peng, C. Baichao, T. Cuihua, B. Sun, M. Zhou, and J. Yuan, "A novel neutral electromagnetic hybrid flexible grounding method in distribution networks," *IEEE Trans. Power Del.*, vol. 32, no. 3, pp. 1350–1358, Jun. 2017.

[21] F. Wang, M. Guo, and G. Yang, "Novel arc-suppression methods based on cascaded H-bridge converter," in *Proc. Asia–Pacific Int. Symp. Electromagn. Compat. (APEMC)*, Shenzhen, China, May 2016, pp. 691–694.

[22] W.-Q. Qiu, M.-F. Guo, G.-J. Yang, and Z.-Y. Zheng, "Model-predictive-control-based flexible arc-suppression method for Earth fault in distribution networks," *IEEE Access*, vol. 7, pp. 16051–16065, 2019.



**YANGMING CHEN** was born in Hunan, China, in 1988. He received the B.S. degree in electrical engineering from Southwest Jiaotong University, Chengdu, China, in 2011. He is currently pursuing the Ph.D. degree in electrical engineering with Chongqing University.

His current research interests include cascaded H-bridge inverters and the application of power electronic equipment in distribution networks.



**SHUAI LU** (Member, IEEE) received the B.S.E.E. degree from Chongqing University, Chongqing, China, in 1997, the M.S.E.E. degree from the University of Wisconsin–Milwaukee, Milwaukee, WI, USA, in 2003, and the Ph.D. degree in electrical engineering from the University of Missouri–Rolla, Rolla, MO, USA, in 2007.

In February 2007, he joined MTS Systems Corporation, Eden Prairie, MN, USA, where he was the Lead Power Electronics and Motor Drive Engineer for the successful development of the world's first generation of the hybrid electric system for Formula-1 cars in the 2009 race season (also known as KERS: kinetic energy recovery system), which is arguably the highest power density and performance hybrid electric system in the world. In late 2012, he joined Chongqing University as a Professor, where he has established seven laboratories (two of them are multimegawatts rating test systems) and accomplished numerous industrial research and development projects in various areas of power electronics and motor drives with the particular focus on the applications in hybrid and electric vehicles, and renewable energy systems. During his Ph.D. research, he has authored or coauthored 20 technical articles, including seven IEEE transactions articles.

**XINGDA ZHOU** (Member, IEEE) was born in Jiangsu, China, in 1994. He received the B.S. degree in electrical engineering and the Ph.D. degree in power electronics from Chongqing University, Chongqing, China, in 2015 and 2020, respectively.

He is currently a Researcher with the Institute of Science and Technology, China Three Gorges Corporation. His research interests include LCL filter active damping, three-level inverters, and modular multilevel converter.

**SHIBIN LIANG** was born in Dali, Yunnan, China. He received the B.S. degree from Chongqing University, Chongqing, China, in 1997, and the M.S. degree from the Kunming University of Science and Technology, Kunming, China, in 2008, all in electrical engineering.

He has been a Professorate Senior Engineer at Yunnan Electric Power Test and Research Institute Company, Ltd., since 2016. His current research interests include electrical measurements and power distribution technology.